

Thieno[3,2-b]pyrrole 5-carboxamides as potent and selective inhibitors of *Giardia duodenalis*

Christopher JS. Hart^{a,b,#}, Andrew G. Riches^c, Snigdha Tiash^{a,1}, Rebecca Abraham^d, Keely Fayd'Herbe^{a,b}, Ellis Joch^{a,b}, Bilal Zulfiqar^{a,f}, Melissa L. Sykes^{a,f}, Vicky M. Avery^{a,b,f}, Jan Šlapeta^e, Sam Abraham^d, John H. Ryan^c, Tina S. Skinner-Adams^{a,b,*}

^a Griffith Institute for Drug Discovery, Griffith University, Nathan, Queensland, Australia

^b School of Environment and Sciences, Griffith University, Nathan, Queensland, Australia

^c Commonwealth Scientific and Industrial Research Organization, Biomedical Manufacturing, Clayton, Victoria, Australia

^d Harry Butler Institute, Murdoch University, Western Australia, Australia

^e Sydney School of Veterinary Science, Faculty of Science, University of Sydney, New South Wales, Australia

^f Discovery Biology, Centre for Cellular Phenomics, Griffith University, Nathan, Queensland, Australia

ARTICLE INFO

Keywords:

Giardia duodenalis

Drug discovery

Thieno[3,2-b]pyrrole 5-carboxamides

ABSTRACT

Giardia duodenalis is the causative agent of the neglected diarrhoeal disease giardiasis. While often self-limiting, giardiasis is ubiquitous and impacts hundreds of millions of people annually. It is also a common gastro-intestinal disease of domestic pets, wildlife, and livestock animals. However, despite this impact, there is no vaccine for *Giardia* currently available. In addition, treatment relies on chemotherapies that are associated with increasing failure rates. To identify new treatment options for giardiasis we recently screened the Compounds Australia Scaffold Library for new chemotypes with selective anti-*Giardia* activity, identifying three compounds with sub- μ M activity and promising selectivity. Here we extended these studies by examining the anti-*Giardia* activity of series CL9569 compounds. This compound series was of interest given the promising activity (IC_{50} 1.2 μ M) and selectivity demonstrated by representative compound, SN00798525 (1). Data from this work has identified an additional three thieno [3,2-b]pyrrole 5-carboxamides with anti-*Giardia* activity, including 2 which displayed potent cytotoxic ($IC_{50} \leq 10$ nM) and selective activity against multiple *Giardia* strains, including representatives from both human-infecting assemblages and metronidazole resistant parasites. Preclinical studies in mice also demonstrated that 2 is well-tolerated, does not impact the normal gut microbiota and can reduce *Giardia* parasite burden in these animals.

1. Introduction

The flagellate protozoan, *Giardia duodenalis* (aka *G. lamblia* or *G. intestinalis*) is a neglected, ubiquitous, water-borne parasite that infects humans and a wide range of animals (Riches et al., 2020). While *Giardia* infections may be asymptomatic, they can result in severe and chronic disease, particularly in children (Leung et al., 2019) and young animals (Itoh et al., 2015). Long-term post-infection complications including irritable bowel syndrome and chronic fatigue may also develop (Halliez et al., 2013; Hanevik et al., 2014).

Despite being a common parasite, that has veterinary and public

health significance, there is no vaccine to combat *Giardia*. Treatment options are also limited to a small group of drug classes which have limitations including high treatment failure rates (Riches et al., 2020; Morch et al., 2020), long treatment schedules (Riches et al., 2020), and host gut microbiota impacts (Pilla et al., 2020; Igarashi et al., 2014) that may contribute to post-infection outcomes (Fekete et al., 2020; Singer et al., 2000). As an example, the 5-nitroimidazole metronidazole has reported failure rates of up to 40% in humans (Nabarro et al., 2015) and can significantly decrease the diversity of the host gut microbiota (Pilla et al., 2020), a characteristic that has been linked to poor gut health (Fekete et al., 2020). In addition, the benzimidazole fenbendazole, a

* Corresponding author. Griffith Institute for Drug Discovery, Griffith University, Nathan, Queensland, Australia.

E-mail address: t.skinner-adams@griffith.edu.au (T.S. Skinner-Adams).

Current address: Department of Microbiology and Molecular Genetics, University of California Davis, California, USA.

¹ Current address: Department of Cell Biology and Physiology, Washington University, St. Louis, USA.

commonly recommended treatment agent for *Giardia* infection in animals, was recently reported to have a therapeutic efficacy of 35% in dogs (Kaufmann et al., 2022). To improve treatment options for *Giardia* infections, new therapies that are effective against drug resistant parasites without collateral microbiota impacts are needed.

To identify new treatment options for giardiasis, our group recently assessed the Compounds Australia Scaffold Library for new chemotypes with selective anti-*Giardia* activity (Hart et al., 2022). In this work we extended these studies by examining the anti-*Giardia* activity of series CL9569 compounds. This compound series was not examined in the original study, but representative compound SN00798525 (**1**) demonstrated promising potency (IC_{50} 1.2 μ M) and selectivity for *Giardia* parasites over human cells (IC_{50} > 10 μ M) and bacteria (IC_{50} > 50 μ M) (Hart et al., 2022). To build on this work, we assessed the remaining Compounds Australia CL9569 scaffold compounds for anti-*Giardia* activity. Selected compounds with *in vitro* activity against *Giardia* parasites were also repurchased and synthesized to confirm activity. Given the promising nM *in vitro* growth inhibitory activity displayed by **2** against *Giardia* trophozoites, additional biological assessments, including *in vivo* tolerability and efficacy assessments were carried out with this compound.

2. Methods

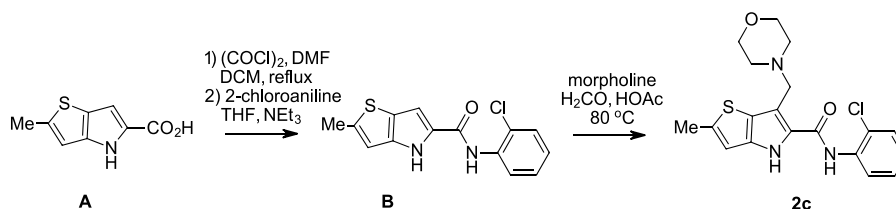
2.1. Chemistry

Melting points were determined on Büchi B-545 digital melting point apparatus and are uncorrected. NMR spectra were recorded in d_6 -DMSO on a Bruker Avance 400 MHz NMR spectrometer with the sample held at 25 ± 0.1 °C. Chemical shifts were referenced using the Unified Scale relative to residual DMSO. Thin layer chromatography (TLC) was performed on Merck pre-coated 0.25 mm silica F₂₅₄ aluminium-backed plates (#5554). Column chromatography was performed using Merck (#9385, 230–400 mesh) silica gel 60. Analytical LCMS was performed on a Waters Acquity I Class with an Acquity UPLC BEH C₁₈ 1.7 mm 2.1 \times 50 mm column with PDA (254 nm) and QDa detection. Mobile phase: H₂O (0.1% formic acid): ACN (0.1% formic acid) 95:5 \rightarrow 100:0 over a 7 min runtime and a flowrate of 0.4 mL/min. Injection volume 1.00 mL. Mass spectrometric analyses were performed on a Thermo Scientific Q Exactive mass spectrometer fitted with an APCI ion source or an ASAP ion source. Positive and/or negative ions were recorded in an appropriate mass range at 140,000 mass resolution. The APCI probe was used without flow of solvent. The nitrogen nebulizing/desolvation gas used for vaporization was heated to 450 °C in these experiments. The sheath gas flow rate was set to 25, the auxiliary gas flow rate to 10 and the sweep gas flow rate to 5 (all arbitrary units). The discharge current was 4 μ A and the capillary temperature was 320 °C. All anhydrous reactions were performed under a dry nitrogen atmosphere. All inorganic solutions are aqueous unless otherwise specified.

Albendazole (ABZ), metronidazole (MTZ), chloroquine (CQ), ampicillin (AMP) and nifurtimox (NFX) were obtained from Sigma, Aldrich (an affiliate of Merck KGaA, Darmstadt, Germany). Amphotericin B (AMB) was obtained from Cayman Chemicals (Ann Arbor, Michigan, USA). CL9569 scaffold compounds were obtained in 100% DMSO as 5 mM stocks from Compounds Australia (Griffith University, Nathan,

Brisbane Australia) where they were stored under robust environmental conditions (Simpson et al., 2014). Compounds **1** and **2** were purchased from ChemDiv (San Diego, California, USA; M372-0589, and M372-0608 respectively) for additional assays (**1b** and **2b**, respectively). Compound **2b** was 98.4% pure by LCMS analysis. Compound **2** was also synthesized according to Scheme 1 to confirm activity (**2c**). Compound **2c** was obtained as a crystalline solid in 96.8% purity (LCMS analysis) and was stable to storage under ambient conditions for several months.

2-Methyl-4H-thieno [3,2-*b*]pyrrole-5-carboxylic acid (**A**) was prepared in three steps from 5-methylthiophene-2-carbaldehyde, as previously described (Heffernan Michele et al., 2007). 2-Methyl-4H-thieno [3,2-*b*]pyrrole-5-carboxylic acid (**A**, 831 mg, 4.59 mmol) was suspended in CH₂Cl₂ (20 mL) then dry dimethylformamide (DMF) (1 drop) and oxalyl chloride (1.16 g, 9.17 mmol) were added. After bubbling had subsided, the mixture was refluxed for 4 h then evaporated to give the acid chloride derivative of **A** as a colourless oil. The acid chloride (654 mg, 3.28 mmol) was dissolved in dry tetrahydrofuran (THF) (5 mL) and this solution was added to a vial containing 2-chloroaniline (460 mg, 3.60 mmol) and triethylamine (996 mg, 9.84 mmol). The mixture was stirred at room temperature for 18 h, then poured into a mixture of sat. NaHCO₃ (20 mL) and EtOAc (20 mL) and stirred vigorously for 10 min. The resulting suspension was filtered and the collected solid washed with water (2 \times 5 mL) and dried to afford *N*-(2-chlorophenyl)-2-methyl-4H-thieno [3,2-*b*]pyrrole-5-carboxamide (**B**, 690 mg, 72%). LCMS: t_R = 3.30 min (88.8% purity) m/z = 291.1 [M+H]⁺. HRMS (APCI, +ve ion) m/z calcd for C₁₄H₁₂ON₂³⁵Cl³²S [M + H]⁺ 291.0353, found 291.0353. ¹H NMR (400 MHz, DMSO-*d*₆) δ 11.77 (brs, 1H); 9.65 (brs, 1H); 7.64 (dd, J = 8.0, 1.4 Hz, 1H); 7.54 (dd, J = 8.0, 1.3 Hz, 1H); 7.40–7.35 (m, 1H); 7.30–7.23 (m, 2H); 6.74 (brs, 1H); 2.50 (brs, 3H). ¹³C NMR (100 MHz, DMSO-*d*₆) δ 159.4, 142.2, 140.9, 134.9, 129.5, 128.8, 128.5, 128.0, 127.5, 126.9, 121.4, 110.3, 103.9, 16.6. Morpholine (50 mg, 0.574 mmol) was added to acetic acid (3 mL) in a microwave vial, followed by aqueous formaldehyde (37% w/w, 47 mg, 0.574 mmol). A solution of *N*-(2-chlorophenyl)-2-methyl-4H-thieno [3,2-*b*]pyrrole-5-carboxamide (**B**, 167 mg, 0.574 mmol) in acetic acid (2 mL) was added and the vial was sealed and heated to 80 °C for 3.5 h (reaction complete by LCMS monitoring). The mixture was cooled and poured into ice-cold 2 M NaOH (20 mL) and extracted into CHCl₃ (3 \times 20 mL). The combined extracts were washed with brine (20 mL), dried (Na₂SO₄) and evaporated to give a yellow solid. The crude product was purified by silica gel chromatography (EtOAc/CHCl₃, 0:100 \rightarrow 10:90) followed by trituration with CHCl₃/methyl *tert*-butyl ether to give *N*-(2-chlorophenyl)-2-methyl-6-(morpholinomethyl)-4H-thieno [3,2-*b*]pyrrole-5-carboxamide **2c** (148 mg, 66%) as a pale yellow solid. M. p. 238–241 °C (decomp.). LCMS: t_R = 1.95 min (96.8% purity) m/z = 390.3 [M+H]⁺. HRMS (APCI, +ve ion) m/z calcd for C₁₉H₂₁O₂N₃³⁵Cl³²S [M + H]⁺ 390.1038, found 390.1037. ¹H NMR (400 MHz, CDCl₃) δ 11.55 (brs, 1H); 9.60 (brs, 1H); 7.87 (dd, J = 8.1, 1.5 Hz, 1H); 7.43 (dd, J = 8.0, 1.4 Hz, 1H); 7.33–7.28 (m, 1H); 7.16–7.11 (m, 1H); 6.62–6.59 (m, 1H); 3.77 (s, 2H), 3.68–3.62 (m, 4H); 2.64–2.55 (m, 4H); 2.54 (d, J = 1.1 Hz, 3H). ¹³C NMR (100 MHz, *d*₆-DMSO) δ 159.8, 142.2, 139.0, 135.0, 129.5, 127.5, 127.4, 126.9, 126.43, 126.36, 124.1, 113.1, 110.6, 65.8, 54.2, 52.5, 16.6.



Scheme 1. Preparation of **2c**.

2.2. *In vitro* culture of *G. duodenalis*

G. duodenalis parasites including the assemblage A strain BRIS/87/HEPU/713 (Nolan et al., 2011) and the assemblage B strain BRIS/91/HEPU/1279 (Nolan et al., 2011) were maintained in sealed cultures tubes, using modified Keisters TYI-S-33 medium supplemented with 10% heat-inactivated foetal bovine serum (FBS), 100 units/mL penicillin, and 100 µg/mL streptomycin as previously described (Keister, 1983). MTZ resistant (BRIS/91/HEPU/1279m1 (Tejman-Yarden et al., 2013)) parasites were maintained on 15 µM MTZ which was removed two days prior to compound activity assessments.

2.3. *G. duodenalis* compound susceptibility assays

The activity of compounds against *Giardia* parasites was assessed via automated microscopy as previously described (Hart et al., 2017). Due to the limited amount of compound available from Compounds Australia, the activity of CL9569 compounds was assessed in duplicate in dose response (minimum of eight dilutions) from 10 µM, whereas compounds purchased from ChemDiv or synthesized were assessed in triplicate. Media, parasites in media, and DMSO-vehicle controls were included on each plate and an ABZ or MTZ positive control plate was run with each assay. Growth inhibition was calculated as a percentage relative to vehicle controls minus media background and IC₅₀ values were determined using non-linear regression curve analysis (variable slope, 4 parameters; GraphPad Prism). Minimum lethal concentration (MLC) assessments were performed as previously described (Hart et al., 2022) with all experiments conducted at least three times in duplicate.

2.4. Mammalian cell culture and compound susceptibility assays

Neonatal Foreskin Fibroblasts (NFF) and Human Embryonic Kidney (HEK-293) cells were maintained in RPMI-1640 supplemented with 10% FBS, 100 units/mL penicillin, and 100 µg/mL streptomycin, in cell culture flasks (Corning, USA). The selectivity of compounds demonstrating activity against *Giardia* parasites (IC₅₀ < 10 µM) was assessed against NFF as previously described using sulforhodamine B (Chua et al., 2021). Compounds provided by Compounds Australia were assessed in duplicate on two separate occasions, whereas synthesized compounds or compounds purchased from ChemDiv were tested at least three times in triplicate. Given the promising anti-*Giardia* activity of **2** the activity of this compound against HEK-293 cells was also assessed. All 96-well test plates included media only (background), negative (no compound and no vehicle) and vehicle (DMSO) controls. A CQ positive control plate was included in each assay. Growth inhibition was calculated relative to vehicle controls minus background, and when possible IC₅₀ values were determined using non-linear regression curve analysis (variable slope, 4 parameters; GraphPad Prism). Selectivity indices (SI) were calculated as previously described (Katsuno et al., 2015).

2.5. *Plasmodium* culture and compound susceptibility assays

Plasmodium falciparum 3D7 parasites were maintained in ORh⁺ human erythrocytes in RPMI 1640 supplemented with 10% heat inactivated human serum, 50 µg/mL hypoxanthine and 5 mg/L gentamycin at 37 °C in 5% O₂ and 5% CO₂ in N₂ essentially as previously described (Trager et al., 1976). The activity of **1** and **2** was assessed against 3D7 *P. falciparum* asexual erythrocytic parasites in 48 h [³H]-hypoxanthine incorporation assays as previously described (Skinner-Adams et al., 2019). All 96-well test plates included uninfected RBC background controls, negative (no compound and no vehicle) and vehicle (DMSO) controls. Percentage growth inhibition was calculated relative to matched vehicle controls minus background counts. At least two independent assays, in triplicate, were performed for each compound, with CQ included as the positive control in each assay.

2.6. *Leishmania* culture and compound susceptibility assays

Leishmania donovani promastigote parasites (MHOM/IN/80/DD8, ATCC 50212) were maintained in modified M199 Hanks salt medium (pH 6.8) supplemented with 10% heat inactivated FBS at 27 °C. Parasites were sub-cultured every 7 days at a concentration of 1 × 10⁵ cells/mL. THP-1 cells (human monocytic leukemia cell line, ATCC TIB202) were maintained in RPMI supplemented with 10% FBS at 37 °C in 5% CO₂ and sub-cultured every two to three days to maintain a cell density of 2 × 10⁵ to 1 × 10⁶ cells/mL. THP cells were differentiated into macrophages in the 384 well microtiter plates using phorbol 12-myristate 13-acetate (PMA) (Duffy et al., 2017). The activity of **1b** and **2b** was assessed against *L. donovani* DD8 amastigotes essentially as previously described (Duffy et al., 2017) where transformed THP-1 cells were infected with metacyclic promastigotes (1:5 ratio of host versus parasite cells) and exposed to compounds for 96 h. Cells were then fixed (4% paraformaldehyde), stained with SYBR green and CellMask Deep Red (Thermo-Fisher Scientific, Waltham, MA) and imaged using the Opera high-content imaging system (PerkinElmer) with a 20x water objective to determine growth inhibition. Image analysis was performed using Acapella version 2.6. Initially, segmentation of nuclear and cell boundaries was used to identify the region of host cell cytoplasm, followed by spot detection to identify parasites within the cytoplasm of the cell. An infected cell was defined as a host cell containing > three parasites within the cytoplasmic region. AMB at a concentration of 2 µM was included as a positive control and negative vehicle (0.4% DMSO) wells were included on all assay plates. The final assay concentrations of test compounds ranged from 80 µM to 0.004 µM. Each compound was assessed twice in triplicate and where possible IC₅₀ values were calculated using non-linear regression (variable slope, 4 parameters; GraphPad Prism).

2.7. *T. cruzi* *in vitro* sub-culture and compound susceptibility assays

Trypanosoma cruzi Tulahuen strain parasites were maintained in 3T3 (mouse embryo fibroblast; ATCC CCL92) cells in RPMI medium with no phenol red, supplemented with 10% FBS as previously described (Sykes et al., 2015). Parasites were sub-cultured by infecting new 3T3 cultures with freshly egressed *T. cruzi* trypomastigotes from the supernatant of a flask of previously infected 3T3 cells (Sykes et al., 2015). The activity of **1b** and **2b** against *T. cruzi* intracellular amastigotes was determined with an *in vitro* imaging assay, utilising an Opera image-based system as previously described (Sykes et al., 2015). Each compound was assessed in single point, over three experimental replicates. The final assay concentrations of test compounds ranged from 73.2 µM to 3.7 × 10^{−4} µM. Puromycin was utilised as a positive control for 3T3 host cells at a final assay concentration of 30 µM and 12 µM NFX was used as the positive control for *T. cruzi* intracellular amastigotes. The IC₅₀ values of control compounds and where possible test compounds were calculated using non-linear regression (variable slope, 4 parameters) in GraphPad Prism.

2.8. Antibacterial activity assessments

The activity of compound **1b** and **2b** against *Enterococci faecalis* (ATCC 29212), *Staphylococcus aureus* (ATCC 29213) and *Escherichia coli* (ATCC 25922) was assessed according to Clinical Laboratory Standards Institute guidelines for microbroth dilutions using LB broth (CLSI, 2015). AMP was used as a positive control. Each 20 mM solution of test compound was diluted in LB broth for testing and all test organisms were exposed to compounds for 20 h before growth inhibition was assessed to identify minimum inhibitory concentrations.

2.9. *In vivo* tolerability assessments

The *in vivo* tolerability of **2c** was assessed in female outbred Swiss

mice (Animal Research Centre, Perth Australia, ethics approval ESK/01/17/AEC and GRIDD/03/21/AEC (Griffith University approved April 10, 2017 and March 21, 2021 respectively) using the dose escalation protocol previously described (Hart et al., 2022). Groups of three mice were used to assess increasing doses of each compound and all mice were assessed for adverse effects for seven days post compound administration. Mice were euthanized after observations and samples were collected for pathology assessment. The highest dose assessed was 7.4 mg/kg daily for three days.

2.10. In vivo efficacy studies

The *in vivo* efficacy of **2c** was examined in outbred Swiss mice (Animal Research Centre, Perth Australia, ethics approval AE187, Harry Perkins Institute of Medical Research) as previously described (Abraham et al., 2018). In brief, groups of ten, seven-day-old pups were infected with 10⁵ BAH2c2 trophozoites (100 µL in 0.9% saline) via oral gavage and infections were monitored via the collection of daily faecal samples. Cysts were isolated from faecal samples using centrifugal flotation, resuspended in 500 µL water and counted using Giardi-a-Glo (Sapphire Biosciences, Australia) and a BX-41 immunofluorescent microscope (Olympus, Japan). Once infections were confirmed, approximately 1 week after the oral administration of trophozoites, mice were treated with vehicle, **2c** or MTZ once daily for three days via oral gavage. The day following the final treatment, mice were euthanized and the small intestine removed for trophozoite assessment via manual counting as previously described (Abraham et al., 2018). The large intestine was also removed from each mouse and assessed for cysts. Cyst load was determined using immunofluorescent microscopy as described for faecal samples and data presented as cyst load/gram faeces. Data were processed using Strata version 16.1 with efficacy calculated according to the World Association for the Advancement of Veterinary Parasitology Guidelines (Geurden et al., 2014). Statistical differences between individual groups was assessed using a student t-test in GraphPad Prism.

2.11. Microbiome assessments

The impact of **2c** on the microbiome of 7-week-old outbred Swiss mice was examined in accordance with ethics approval (AE118, Harry Perkins Institute of Medical Research). In brief, three groups of 12 mice (Animal Resource Centre, Perth Australia) were treated with vehicle control, MTZ (100 mg/kg) or **2c** (7.4 mg/kg) daily for three days (day 1, 2 and 3). Faecal samples were collected from individual animals on day 0–5 and stored at room temperature in 80% ethanol. At the completion of the trial approximately 0.2 g of each faecal sample was homogenised in tubes containing glass beads and lysis buffer (FastPrep® 24 homogenizer; MP Biomedicals, Australia; setting 6.0 m/s for 40 s) and a magnetic bead based nucleic acid isolation kit, (MagAttract Power Microbiome DNA/RNA Kit; 27600-4-KF, Qiagen, Australia), adapted for the KingFisher™ Duo (Thermo Scientific™, Australia) was used to isolate DNA from these preparations. DNA samples were subjected to microbial diversity profiling at the Australian Genome Research Facility (Brisbane, Australia). Sequencing of the V3–V4 region of the 16 S rRNA gene was performed on Illumina MiSeq (300 bp pair-end) using primers 341 F (5'-CCT AYG GGR BGC ASC AG-3') and 806 R (5'-GGA CTA CNN GGG TAT CTA AT-3'). Sequence reads were processed using Quantitative Insights into Microbial Ecology (QIIME 1.9.1). Singletons or unique reads in the data set were discarded. Sequences were clustered followed by chimera filtered using “rdp_gold” database as reference. To obtain number of reads in each operational taxonomic unit (OTU), reads were mapped back to OTUs with a minimum identity of 97%. Taxonomy was assigned using QIIME and Greengenes database5 (Version 13.8, Aug 2013).

Multivariate analytical procedures were used to investigate patterns of variation in the composition of bacterial assemblages among faecal samples from mice. The microbiome abundance matrix with taxonomy

of each OTU and sample associated factors were imported for multivariate statistical analysis in PRIMER v7 (Clarke et al., 2015). The data matrix of OTU abundances (or chosen taxonomical level abundance) was fourth-root-transformed. Variation in the structure of bacteria in the mice post intervention was examined on the basis of Bray-Curtis similarity. Analysis of similarities (ANOSIM (Clarke, 1993); was used to test the null hypothesis of no differences among the communities of defined groupings (significance level, $P = 0.05$). Non-metric multidimensional scaling (NMDS) ordination (Kruskal et al., 1978) was undertaken to visualize and explore the patterns of community similarities amongst samples.

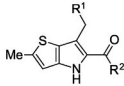
3. Results

3.1. Antigiardial activity and selectivity of the CL9569 scaffold set

Given the activity of **1** in previously published anti-*Giardia* activity assays (Hart et al., 2022), the anti-*Giardia* activity of all CL9569 scaffold compounds was assessed against assemblage B BRIS/91/HEPU/1279 trophozoites. These experiments identified three additional compounds within series (**2**, **3** and **12**; Table 1) with activity (IC₅₀ values ≤ 10 µM) against *G. duodenalis* trophozoites. The most potent of these compounds **2** (IC₅₀ 0.31 µM; Table 1) and **3** (IC₅₀ 0.94 µM) were more active than the original hit compound (**1**; IC₅₀ 1.2 µM; Table 1). The remaining active compound, **12** was less active than all tested compounds (IC₅₀ 5.7 µM). However, all hits demonstrated selectivity for *Giardia* over mammalian cells with no inhibitory activity detected at any of the maximum concentrations assessed (Table 1).

While the small sub-set of scaffold compounds available in Compounds Australia limited structure activity relationship assessments, data demonstrated a requirement for an ortho-substituted *N*-aryl amide in position R² (see Table 1). All other R² functional groups (benzylic, and aliphatic) were inactive. The most potent analogue contained a chlorine ortho to the anilide *N* (compound **2**; 0.31 µM; Table 1). Compounds with ortho methyl (**1**; IC₅₀ 1.2 µM; Table 1), and methylthio (**3**; IC₅₀ 0.94 µM; Table 1) groups were less active. Active compounds also contained a morpholine ring in the R¹ position (Table 1). The only exception to this was compound **12** (R¹ = dimethylamino; IC₅₀ 5.7 µM; Table 1), although this compound also had an additional fluoro substituent in the aryl ring compared to **2**.

Given the activity displayed by multiple CL9569 series analogues, compounds **1** and **2** were purchased from ChemDiv to confirm activity. As an additional mechanism to validate activity and compound identity (Riches et al., 2022), compound **2** was also synthesized and all batches re-assessed against *Giardia* trophozoites *in vitro*. Data from these assays confirmed the anti-*Giardia* activity of **1** and **2** (Table 2). However, follow up activity data suggested that the purchased (**2b**) and freshly synthesized (**2c**) batches of **2** were more potent (IC₅₀ 8.6–12 nM; Table 2) than had been suggested by original work with **2** obtained from Compounds Australia (IC₅₀ 0.31 µM; Table 1). This was likely due to the high inter-assay variability seen with the data obtained in original studies (Table 1), noting that further samples could not be obtained from Compounds Australia for additional assays and this variability was not seen with purchased or freshly synthesized **2** (Table 2), which were used in subsequent studies. The activity of repurchased **1** in these assays (IC₅₀ 0.86 µM Table 2) was not statistically different to that demonstrated by the **1** provided by Compounds Australia (IC₅₀ 1.2 µM; Table 1). Follow up cytotoxicity studies with **1** and **2** against NFF and HEK293 cells were encouraging (less than 50% growth inhibition at 100 µM in all cases; not shown), with favourable selectivity indices of >116 and > 8333 respectively. Likewise, the assessment of these compounds against bacteria (Table 2) and against additional *G. duodenalis* parasites, including assemblage A (BRIS/87/HEPU/713 IC₅₀ 10 nM; Fig. 1b and c) and MTZ resistant parasites (BRIS/91/HEPU/1279m1 IC₅₀ 5.5 nM; Fig. 1b and c) were encouraging demonstrating that the selective activity of **2** for parasites is retained against multiple assemblages and MTZ

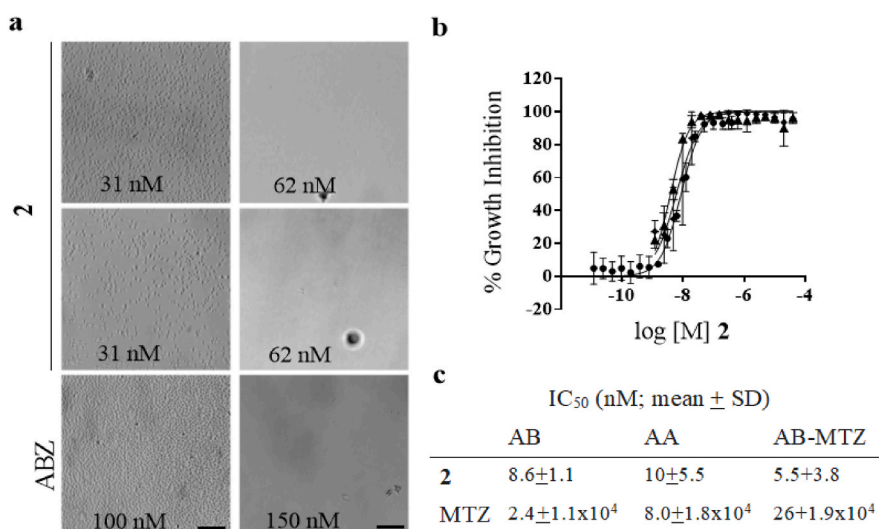
Table 1The *in vitro* anti-*Giardia* activity and selectivity of CL9569 compounds.


Compound	R ¹	R ²	IC ₅₀ (M; mean ± SD) ^b		Selectivity
			<i>Giardia</i> (48h)	NFF	
1 ^a			1.2x10 ⁻⁶ ± 4.0x10 ⁻⁹	>2.0x10 ⁻⁵	>16
2			3.1x10 ⁻⁷ ± 2.5x10 ⁻⁷	>1.0x10 ⁻⁵	>32
3			9.4x10 ⁻⁷ ± 2.3x10 ⁻⁷	>2.0x10 ⁻⁵	>21
4			>1.0x10 ⁻⁵	nd	nd
5			>1.0x10 ⁻⁵	nd	nd
6			>1.0x10 ⁻⁵	nd	nd
7			>1.0x10 ⁻⁵	nd	nd
8			>1.0x10 ⁻⁵	nd	nd
9			>1.0x10 ⁻⁵	nd	nd
10			>1.0x10 ⁻⁵	nd	nd
11			>1.0x10 ⁻⁵	nd	nd
12			5.7x10 ⁻⁶ ± 3.1 x10 ⁻⁷	>2.0x10 ⁻⁵	>3
13			>1.0x10 ⁻⁵	nd	nd
14			>1.0x10 ⁻⁵	nd	nd
15			>1.0x10 ⁻⁵	nd	nd
16			>1.0x10 ⁻⁵	nd	nd
17			>1.0x10 ⁻⁵	nd	nd
18			>1.0x10 ⁻⁵	nd	nd
19			>1.0x10 ⁻⁵	nd	nd
20 ^a			>1.0x10 ⁻⁵	nd	nd
21			>1.0x10 ⁻⁵	nd	nd
22			>1.0x10 ⁻⁵	nd	nd
23			>1.0x10 ⁻⁵	nd	nd
24			>1.0x10 ⁻⁵	nd	nd
25			>1.0x10 ⁻⁵	nd	nd
26			>1.0x10 ⁻⁵	nd	nd
27			>1.0x10 ⁻⁵	nd	nd
28			>1.0x10 ⁻⁵	nd	nd
29			>1.0x10 ⁻⁵	nd	nd
ABZ			5.7x10 ⁻⁸ ±1.7x10 ⁻⁸	1.1x10 ⁻⁶ +2.8x10 ⁻⁷	19.3
CQ			nd	3.1x10 ⁻⁵ +2.2x10 ⁻⁵	nd

^a Data from original screen assessments [13]; nd, not determined.^b Where an IC₅₀ could not be determined the IC₅₀ is reported as > than highest concentration tested

Table 2The *in vitro* activity of 1 and 2 against selected pathogens.

Compound	IC ₅₀ (M; mean ± SD) ^b				MIC (M)		
	<i>Giardia</i> AB ^a	<i>P. falciparum</i>	<i>L. donovani</i>	<i>T. cruzi</i>	<i>E. faecalis</i>	<i>E. coli</i>	<i>S. aureus</i>
2b	$1.2 \times 10^{-8} \pm 8.4 \times 10^{-9}$	$>5.0 \times 10^{-5}$ (2.0%)	$>8.0 \times 10^{-5}$	$>7.3 \times 10^{-5}$	$>2.0 \times 10^{-4}$	$>2.0 \times 10^{-4}$	$>2.0 \times 10^{-4}$
2c	$8.6 \times 10^{-9} \pm 1.1 \times 10^{-9}$	nd	nd	nd	nd	nd	nd
1b	$8.2 \times 10^{-7} \pm 2.2 \times 10^{-7}$	$>5.0 \times 10^{-5}$ (42%)	$>8.0 \times 10^{-5}$ (39%)	$>7.3 \times 10^{-5}$	$>2.0 \times 10^{-4}$	$>2.0 \times 10^{-4}$	$>2.0 \times 10^{-4}$
ABZ	$5.7 \times 10^{-8} \pm 1.7 \times 10^{-8}$	nd	nd	nd	nd	nd	nd
CQ	nd	$1.4 \times 10^{-8} \pm 6.4 \times 10^{-9}$	nd	nd	nd	nd	nd
AMB	nd	nd	$8.7 \times 10^{-8} \pm 2.0 \times 10^{-9}$	nd	nd	nd	nd
NFX	nd	nd	nd	$9.8 \times 10^{-7} \pm 8.3 \times 10^{-8}$	nd	nd	nd
AMP	nd	nd	nd	nd	$<3.7 \times 10^{-5}$	$<3.7 \times 10^{-5}$	$<3.7 \times 10^{-5}$

^a Assemblage B *G. duodenalis* BRIS/91/HEPU/1279 parasites.^b Where an IC₅₀ could not be determined but inhibition was seen, the highest concentration tested is provided with the average % inhibition, when no inhibition was observed the IC₅₀ is reported as > then highest concentration tested.**Fig. 1.** Compound 2 demonstrates potent activity against *G. duodenalis* trophozoites.

resistant parasites (Fig. 1b and c). Moreover, experiments examining the minimum lethal concentration (MLC) of 2 demonstrated that this compound kills parasites at nM concentrations (MLC 62 nM; Fig. 1a). The MLC of ABZ in these assays (Fig. 1a; MLC 150 nM) was in line with previously reported values (Cedillo-Rivera et al., 1992).

The MLC of resynthesised 2 and ABZ was assessed against BRIS/91/HEPU/1279 trophozoites (a). Parasites were exposed to compounds for 48 h in 96-well flat-bottom plates before being returned to culture for a further four days and imaged to assess growth. Brightfield images were taken with a 10× widefield objective on an IX-73 microscope (Olympus, Japan; scale bar 100 µm). Image brightness was adjusted using Image J (NIH, USA). Dose response assays were performed to examine the 48 h activity of 2 against BRIS/91/HEPU/1279 assemblage B (AB; circles), BRIS/87/HEPU/713 assemblage A (AA; diamonds) and the MTZ resistant assemblage B BRIS/91/HEPU/1279m1 parasites (AB-MTZ; triangles) (b) and IC₅₀ values were determined using non-linear regression (c). All experiments were performed at least three times in triplicate.

3.2. Activity against *P. falciparum*, *L. donovani* and *T. cruzi*

To determine whether 2 and 1 have activity against additional parasites the inhibitory activity of these compounds was assessed against *P. falciparum*, *L. donovani* and *T. cruzi*. While data showed some inhibition with 1 at high concentrations against *P. falciparum* (42% at 50 µM) and *L. donovani* (39% at 80 µM), both compounds demonstrated limited activity against all additional parasites tested (<50% growth inhibition

in all cases, Table 2).

3.3. In vivo tolerability and efficacy

Given the potent *in vitro* activity of 2, proof-of-concept *in vivo* studies were performed. First the *in vivo* tolerability of 2 was assessed in uninfected female outbred Swiss mice (Animal Research Centre, Perth Australia). No adverse signs or pathology were observed following single oral doses of 2 for 3 days at concentrations up to 7.4 mg/kg, the maximum dose assessed.

To assess *in vivo* activity, three groups of ten mice infected with *G. duodenalis* were administered 2 (0.74 mg/kg), MTZ (100 mg/kg) or PBS vehicle control for three days. Data from this work, demonstrated that 2 was effective in reducing the cyst and trophozoite burden in mice, by 98.8% ($P < 0.0001$) and 73.5% ($P = 0.006$) as compared to vehicle treated mice respectively (Fig. 2a and b). MTZ, included as a positive control in this experiment was effective in reducing the cyst and trophozoite burden of animals by 65.6 ($P = 0.0003$) and 98.1% ($P < 0.0001$) respectively (Fig. 2a and b). Given this promising result a further study was performed to determine whether a higher dose of 2 (7.4 mg/kg) would cure infections in mice. In this work an additional three groups of ten mice infected with *G. duodenalis* were administered 2 (7.4 mg/kg), MTZ (100 mg/kg) or 50%PBS/DMSO vehicle control daily for three days. The activity of 2 in these studies was less than that observed previously, with this treatment regimen reducing cyst and trophozoite burden in mice, by 80.1% and 54.2% respectively as

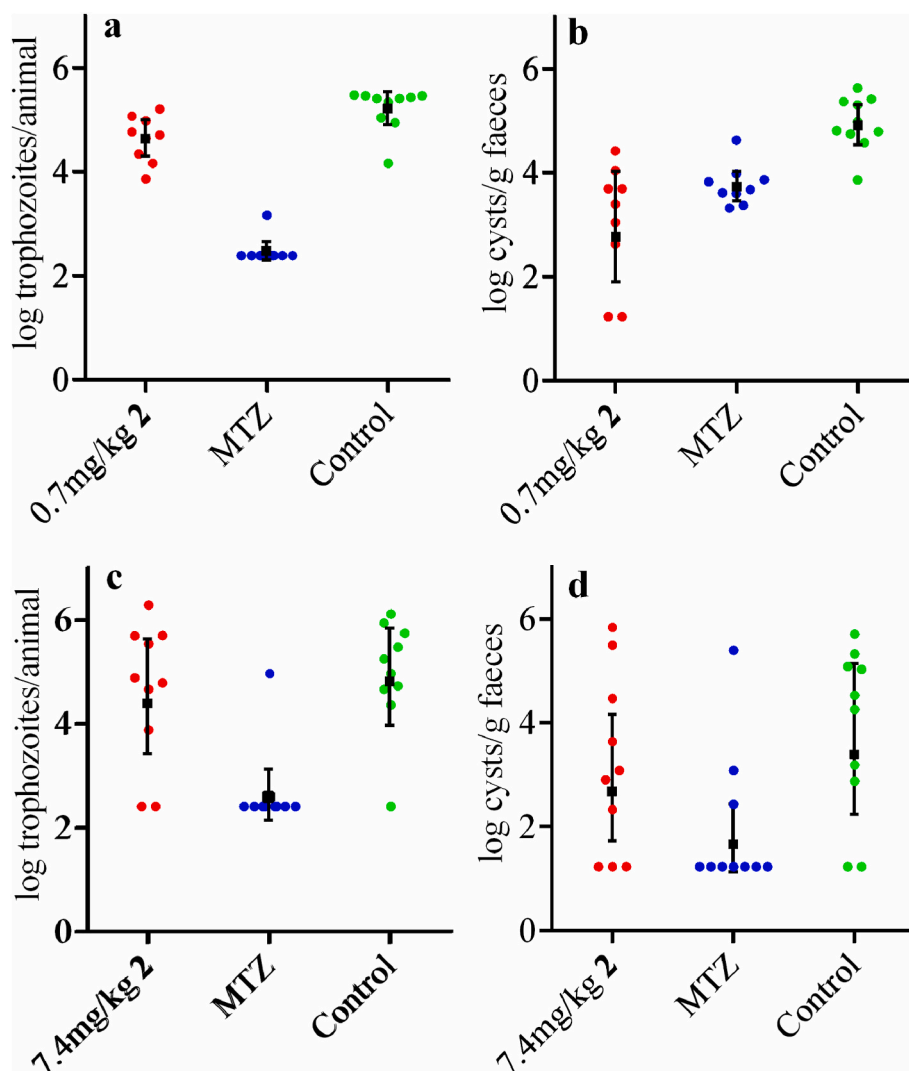


Fig. 2. Compound 2 demonstrates *in vivo* activity in a mouse model of giardiasis.

compared to vehicle treated mice (Fig. 2c and d; $P > 0.05$).

The ability of 0.74 mg/kg 2 (a and b) and 7.4 mg/kg 2 (c and d) to reduce *Giardia* trophozoite (a and c) and cyst burden (b and d) was assessed in outbred Swiss mice. Groups of 10 mice were administered 2, 100 mg/kg MTZ or vehicle control for three days before parasite load was assessed on day four. Bar graphs represent the geometric mean parasite load for each group where error bars are 95% confidence intervals of this mean. Individual animal data are also shown.

3.4. Microbiome assessments

We did not detect any significant ($P < 0.05$) changes in the bacterial profile of mice exposed to compound 2 or vehicle control during the three-day dosing regimen (Fig. 3). However, mice exposed to metronidazole demonstrated a visual shift in profile using MNDs, with significant shift from the vehicle (DMSO/PBS) and compound 2 exposed mice from Day 1–3 (Fig. 3a). This was consistent with a significant ($P < 0.05$) difference in the bacterial profile between mice exposed to metronidazole and those exposed to vehicle (DMSO/PBS) or compound 2 at the bacterial family level (Fig. 3b).

Nucleotide sequence data from this study are available from the National Centre for Biotechnology Information (NCBI) in the SRA database under BioProject accession number: PRJNA990832. PRIMER and associated files are available at LabArchives: <https://dx.doi.org/10.25833/r1ac-rd66>.

10.25833/r1ac-rd66.

Multivariate analysis of mice bacterial profiles at different time-points during the trial. Non-metric MDS ordination (NMDS) plots for bacterial abundance (a) and analysis of similarity (ANOSIM) (b). The ordinations are from abundances at the family level from bacterial OTUs (V3–V4 16 S rRNA gene diversity profiling assay). Histograms of permuted distributions of the test statistics R (up to 999 permutations, ANOSIM; null hypothesis - is no significant difference among communities, $P < 0.05$) with observed R (red line) shown. Group of mice (2, metronidazole, and control) are depicted by shape and colour, and associated number indicates cage number (1–9).

4. Discussion

Despite being one of the most common parasitic organisms of humans and animals, that has veterinary and public health significance there is no vaccine for *Giardia*. Current treatment options are also inadequate, relying on drugs that are associated with resistance and increasing rates of treatment failures (Riches et al., 2020). To improve this situation our group has begun a campaign to identify new anti-*Giardia* chemotypes for therapy development. In the current work we extended our previous study which identified the thieno [3,2-b]pyrrole 5-carboxamide 1 as an anti-*Giardia* agent (Hart et al., 2022), to determine if this scaffold warrants further investigation as a source of new

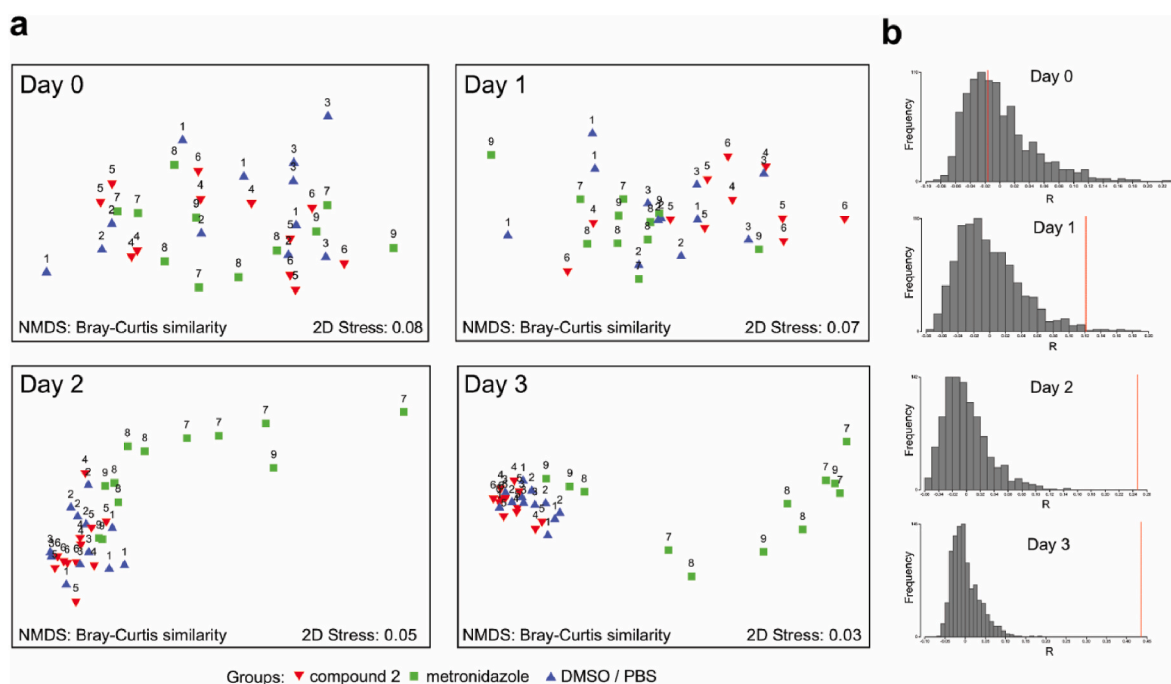


Fig. 3. Impact of 2 on the faecal microbiome of mice.

anti-*Giardia* agents. This follow-up work confirmed the promising anti-*Giardia* activity of **1** and identified additional compounds with anti-*Giardia* activity in the CL9569 Compounds Australia scaffold set ($IC_{50} < 10 \mu M$; Table 1). Studies with additional parasites suggested that the activity of these compounds may be specific to *Giardia* (Table 2), however this work will need to be extended to additional organisms including *Trichomonas* parasites to determine if this is the case. Regardless of host specificity, the identification of multiple thieno [3,2-*b*]pyrrole 5-carboxamides with activity against *G. duodenalis* (Table 1) supported the further investigation of this scaffold as a source of new anti-*Giardia* agents. Additional evidence to support the further investigation of thieno [3,2-*b*]pyrrole 5-carboxamides for their potential as new anti-*Giardia* agents included the potent and selective *in vitro* activity of **2**, which was demonstrated to have low nM, *in vitro* activity against multiple *G. duodenalis* assemblages, including MTZ resistant parasites (IC_{50} 5.5–10 nM; MLC 62 nM; Fig. 1). These *in vitro* inhibitory data demonstrated **2** to be one of the most potent anti-*Giardia* compounds documented to date. Indeed, to the best of our knowledge, the only other molecules that have been shown to have *in vitro* growth inhibitory activity against *G. duodenalis* in this range are fumagillin (IC_{50} 2–10 nM (Kulakova et al., 2014)), which has been associated with *in vivo* toxicity (van den Heever et al., 2014), and selected anti-*Giardia* hybrid molecules, including CMC-20 (IC_{50} 10 nM (Matadamas-Martinez et al., 2016)), which have known and multiple anti-*Giardia* pharmacophores (reviewed in (Riches et al., 2020)).

Compound **2** demonstrated low *in vitro* toxicity against multiple bacteria populations (Table 2). This translated to *in vivo* studies in mice where **2** did not significantly impact the gut microbial diversity of mice (Fig. 3). These data strongly suggest that, unlike MTZ, the thieno [3,2-*b*]pyrrole 5-carboxamide, **2** is unlikely to contribute to host gut dysbiosis via undesirable antibiotic effects when used to combat *Giardia* parasite infection. Crucially, proof-of-concept *in vivo* data demonstrated that **2** can reduce *Giardia* parasite burden in mice. At a low dose of 0.74 mg/kg for three days, **2** reduced *G. duodenalis* trophozoite and cyst burden in mice by 73.5% and 98.8%, respectively. While a higher dose of **2** (7.4 mg/kg daily for three days), did not improve this activity (Fig. 2) these data highlight the potential of this scaffold for further development, suggesting that additional medicinal chemistry and an improved

understanding of structure activity relationships may facilitate the development of new compounds with improved *in vivo* activity. Although the reason for the lower activity of **2** at the higher dose is unclear, this compound's poor aqueous solubility is likely to be a factor. The poor solubility of **2** meant that it was not administered to mice in PBS alone at the higher dose of 7.4 mg/kg (Fig. 2). The high melting point (238–241 °C) of **2** was also indicative of high lattice energy, and hence poor solubility (Ishikawa et al., 2011; Jain et al., 2001). The relatively high $clogD_{7.4}$ of **2** (3.8; calculated using ChemAxon Instant JChem software Version 18.5.0.) may also be a factor. Future analogues should incorporate structural changes likely to improve biorelevant solubility by lowering $clogD_{7.4}$ and/or decreasing the lattice energy of the solid. Structural modifications to improve compound half-life and permeability may also be warranted. Although the importance of these characteristics to the *in vivo* activity of compounds that target gastro-intestinal pathogens remains unclear, the generation and biological assessment of analogues that retain their activity against parasites but have a longer half-life and improved permeability, would help guide lead optimisation, while providing evidence of systemic exposure impact. As the small sub-set of scaffold compounds available in Compounds Australia limited structure activity relationship assessments in the current study, additional analogues should be investigated. Variations to both the bicyclic core and the various substituents may provide analogues with improved physicochemical properties including solubility to provide compounds with improved *in vivo* activity.

To the best of our knowledge the thieno [3,2-*b*]pyrrole 5-carboxamides investigated in this study have not previously been shown to have anti-*Giardia* activity. Related thieno [3,2-*b*]pyrrole 5-carboxamides have been shown to inhibit Chikungunya and other alphaviruses, while exhibiting minimal cytotoxicity (Ching et al., 2015). While compounds with a thieno [3,2-*b*]pyrrole core inhibit hepatitis C virus RNA polymerase (Ontoria et al., 2006; Martin Hernando et al., 2009), *G. duodenalis* does not produce an RNA-dependant RNA polymerase, and there is no significant amino acid similarity between this enzyme and any protein predicted to be encoded in the *G. duodenalis* genome (BLAST E-scores all >1; data not shown), suggesting different mechanisms of action in the two pathogens. While additional studies with multiple resistant lines should be performed to confirm findings, the potent

activity of **2** against multiple *G. duodenalis* assemblages including MTZ resistant parasites suggests a different mode of action to the 5-nitroimidazoles. The observation that low-dose **2** reduced host cyst shedding by 98.8% (Fig. 2) was also interesting and may translate to reduce parasite transmission. While the specific biochemical target(s) of thieno [3,2-b] pyrrole-5-carboxamides such as **2** in *Giardia* parasites remains to be determined, further investigations would guide medicinal chemistry efforts to optimise *in vivo* activity. Studies to investigate the interactions of these compounds with other anti-*Giardia* agents should also be pursued to investigate the potential of these compounds as combination partners with current drugs to combat drug resistant parasites and prevent therapeutic failures.

The current study has demonstrated that some thieno [3,2-b]pyrrole-5-carboxamides have *in vitro* anti-*Giardia* activity as well as promising *in vivo* activity. This chemotype therefore warrants further investigation as a new class of anti-*Giardia* agent. Further exploration of the structure activity relationships in this series are required to improve *in vivo* activity with the objective of achieving parasite cures. Further studies to investigate the mechanism by which these compounds kill parasites may help to identify potential therapeutic partners and monitoring strategies that will aid in combating drug resistant parasites into the future.

Declarations of competing interest

CJS Hart, AG Riches, JH Ryan, and TS Skinner-Adams, are inventors on a PCT application that covers small molecule compounds derived from the compounds discussed in this manuscript.

Acknowledgements

We thank the National Health and Medical Research Council of Australia for funding (APP1141069) to TSA, JHR, JŠ, SA, and AR. We thank the Australian Red Cross Lifeblood for the provision of human blood and sera for culture of *Plasmodium* parasites. We acknowledge Compounds Australia (www.compoundsaustralia.com) for their provision of specialised compound management and logistics research services to the project.

References

- Abraham, R.J., et al., 2018. *Giardia duodenalis* mouse model for the development of novel anti-giardial agents. *J. Microbiol. Methods* 145, 7–9.
- Cedillo-Rivera, R., Munoz, O., 1992. *In-vitro* susceptibility of *Giardia lamblia* to albendazole, mebendazole and other chemotherapeutic agents. *J. Med. Microbiol.* 37 (3), 221–224.
- Ching, K.C., et al., 2015. Trisubstituted thieno[3,2-b]pyrrole 5-carboxamides as potent inhibitors of alphaviruses. *J. Med. Chem.* 58 (23), 9196–9213.
- Chua, M.J., et al., 2021. Histone deacetylase inhibitor AR-42 and achiral analogues kill malaria parasites *in vitro* and in mice. *Int J Parasitol Drugs Drug Resist* 17, 118–127.
- Clarke, K., 1993. Non-parametric multivariate analyses of changes in community structure. *Aust. J. Ecol.* 18, 117–143.
- Clarke, K.R., Gorley, R.N., 2015. PRIMER V7: User Manual/Tutorial. PRIMER-E Plymouth.
- CLSI, 2015. M07-A10 Methods for the Dilution Antimicrobial Susceptibility Tests for Bacteria the Grow Aerobically; Approved Standard, tenth ed. CLSI, Wayne, PA.
- Duffy, S., et al., 2017. Screening the medicines for malaria venture pathogen box across multiple pathogens reclassifies starting points for open-source drug discovery. *Antimicrob. Agents Chemother.* 61 (9).
- Fekete, E., et al., 2020. *Giardia* spp. and the gut microbiota: dangerous liaisons. *Front. Microbiol.* 11, 618106.
- Geurden, T., et al., 2014. World Association for the Advancement of Veterinary Parasitology (WAAVP): guideline for the evaluation of drug efficacy against non-coccidial gastrointestinal protozoa in livestock and companion animals. *Vet. Parasitol.* 204 (3–4), 81–86.
- Halliez, M.C.M., Buret, A.G., 2013. Extra-intestinal and long term consequences of *Giardia duodenalis* infections. *World J. Gastroenterol.* 19 (47), 8974–8985.
- Hanevik, K., et al., 2014. Irritable bowel syndrome and chronic fatigue 6 years after giardia infection: a controlled prospective cohort study. *Clin. Infect. Dis.* 59 (10), 1394–1400.
- Hart, C.J., et al., 2017. A novel *in vitro* image-based assay identifies new drug leads for giardiasis. *Int J Parasitol Drugs Drug Resist* 7 (1), 83–89.
- Hart, C.J.S., et al., 2022. A subset screen of the compounds Australia scaffold library identifies 7-acylaminodibenzoxazepinones as potent and selective hits for anti-giardia drug discovery. *Biomedicines* 10 (12).
- Heffernan Michele, L.R., et al., 2007. Fused Heterocyclic Inhibitors of D-Amino Acid Oxidase. SEPRACOR INC.
- Igarashi, H., et al., 2014. Effect of oral administration of metronidazole or prednisolone on fecal microbiota in dogs. *PLoS One* 9 (9), e107909.
- Ishikawa, M., Hashimoto, Y., 2011. Improvement in aqueous solubility in small molecule drug discovery programs by disruption of molecular planarity and symmetry. *J. Med. Chem.* 54 (6), 1539–1554.
- Itoh, N., et al., 2015. Prevalence of intestinal parasites in breeding kennel dogs in Japan. *Parasitol. Res.* 114 (3), 1221–1224.
- Jain, N., Yalkowsky, S.H., 2001. Estimation of the aqueous solubility I: application to organic nonelectrolytes. *J. Pharmacol. Sci. (Tokyo, Jpn.)* 90 (2), 234–252.
- Katsuno, K., et al., 2015. Hit and lead criteria in drug discovery for infectious diseases of the developing world. *Nat. Rev. Drug Discov.* 14 (11), 751–758.
- Kaufmann, H., et al., 2022. Lack of efficacy of fenbendazole against *Giardia duodenalis* in a naturally infected population of dogs in France. *Parasite* 29, 49.
- Keister, D.B., 1983. Axenic culture of *Giardia lamblia* in TYI-S-33 medium supplemented with bile. *Trans. R. Soc. Trop. Med. Hyg.* 77 (4), 487–488.
- Kruskal, J., Wish, M., 1978. *Multidimensional Scaling*. Quantitative Applications in the Social Science. SAGE Publications, Inc.
- Kulakova, L., et al., 2014. Discovery of novel anti-giardiasis drug candidates. *Antimicrob. Agents Chemother.* 58 (12), 7303–7311.
- Leung, A.K.C., et al., 2019. Giardiasis: an overview. *Recent Pat. Inflamm. Allergy Drug Discov.* 13 (2), 134–143.
- Martin Hernando, J.L., et al., 2009. Optimization of thienopyrrole-based finger-loop inhibitors of the hepatitis C virus NS5B polymerase. *ChemMedChem* 4 (10), 1695–1713.
- Matadamas-Martinez, F., et al., 2016. Proteomic and ultrastructural analysis of the effect of a new nitazoxanide-N-methyl-1H-benzimidazole hybrid against *Giardia intestinalis*. *Res. Vet. Sci.* 105, 171–179.
- Morch, K., Hanevik, K., 2020. Giardiasis treatment: an update with a focus on refractory disease. *Curr. Opin. Infect. Dis.* 33 (5), 355–364.
- Nabarro, L.E., et al., 2015. Increased incidence of nitroimidazole-refractory giardiasis at the hospital for tropical diseases, London: 2008–2013. *Clin. Microbiol. Infect.* 21 (8), 791–796.
- Nolan, M.J., et al., 2011. Barcoding of *Giardia duodenalis* isolates and derived lines from an established cryobank by a mutation scanning-based approach. *Electrophoresis* 32 (16), 2075–2090.
- Ontoria, J.M., et al., 2006. Identification of thieno[3,2-b]pyrroles as allosteric inhibitors of hepatitis C virus NS5B polymerase. *Bioorg. Med. Chem. Lett* 16 (15), 4026–4030.
- Pilla, R., et al., 2020. Effects of metronidazole on the fecal microbiome and metabolome in healthy dogs. *J. Vet. Intern. Med.* 34 (5), 1853–1866.
- Riches, A., et al., 2020. Anti-*Giardia* drug discovery: current status and gut feelings. *J. Med. Chem.* 63 (22), 13330–13354.
- Riches, A.G., H. C., Schmit, M., Debele, E., Tiash, S., Clapper, E., Skinner-Adams, T., Ryan, J.H., 2022. Structural Reassignment of a Dibenz[b,f][1,4]oxazepin-11(10h)-One with Potent Anti-giardial Activity.
- Simpson, M., Poulsen, S.A., 2014. An overview of Australia's compound management facility: the Queensland Compound Library. *ACS Chem. Biol.* 9 (1), 28–33.
- Singer, S.M., Nash, T.E., 2000. The role of normal flora in *Giardia lamblia* infections in mice. *J. Infect. Dis.* 181 (4), 1510–1512.
- Skinner-Adams, T.S., et al., 2019. Cyclization-blocked proguanil as a strategy to improve the antimalarial activity of atovaquone. *Commun. Biol.* 2, 166.
- Sykes, M.L., Avery, V.M., 2015. Development and application of a sensitive, phenotypic, high-throughput image-based assay to identify compound activity against *Trypanosoma cruzi* amastigotes. *Int J Parasitol Drugs Drug Resist* 5 (3), 215–228.
- Tejman-Yarden, N., et al., 2013. A reprofiled drug, auranofin, is effective against metronidazole-resistant *Giardia lamblia*. *Antimicrob. Agents Chemother.* 57 (5), 2029–2035.
- Trager, W., Jensen, J.B., 1976. Human malaria parasites in continuous culture. *Science* 193 (4254), 673–675.
- van den Heever, J.P., et al., 2014. Fumagillin: an overview of recent scientific advances and their significance for apiculture. *J. Agric. Food Chem.* 62 (13), 2728–2737.